Run-to-Run Optimization of Biodiesel Production using Probabilistic Tendency Models: A Simulation Study

Martin F. Luna and Ernesto C. Martínez*

INGAR (CONICET—UTN), Avellaneda 3657, Santa Fe, S3002 GJC, Argentina

Variability of the composition and properties of raw materials used for biodiesel production may cause a loss of productivity, since the same operating conditions give rise to different yields for alternative feedstock sources. The capability to re-optimize the process when the raw materials change may lead to a significant improvement in productivity. For yield optimization, first-principles models of a biodiesel reactor have limited prediction capabilities due to the complex kinetics involving transesterification and saponification reactions, which demands active learning of relevant data through optimal design of experiments. In this work, a Bayesian approach for integrating experimentation with imperfect models is proposed to optimize biodiesel production on a run-to-run basis. Parameter distributions in a probabilistic tendency model for the transesterification of triglycerides are re-estimated using data from a sequence of experiments designed to guide policy improvement. Global sensitivity analysis is used to formulate the optimal sampling strategy in each dynamic experiment as an optimization problem. Results obtained highlight that, even when there are significant errors in the tendency model structure and reduced information content in samples, a significant increase in biodiesel production can be achieved after a handful of runs.

Keywords: biodiesel, modelling for optimization, tendency models, transesterification, uncertainty

INTRODUCTION

Biodiesel is a biomass-based fuel produced from natural triglyceride sources, consisting of alkyl esters.[1] While biodiesel could be a good alternative to conventional diesel fuel, it is not yet competitive enough for widespread use. Minimization of production cost and overall optimization of the biodiesel process are outstanding research goals in process engineering.[2,3] Since raw materials account for 80–90 % of the total production cost, special focus is put into maximizing conversion of triglycerides to methyl esters.[4]

Biodiesel is obtained from natural triglyceride sources through a transesterification reaction.[5] The process uses short chain alcohols to break the triglyceride molecules into alkyl esters (biodiesel) and glycerol (as a byproduct).[6] Homogeneous transesterification with an alkali catalyst seems to be the most popular production method since, depending on the scale, it can be conducted as either a continuous or batch production.[7,8] Batch processes favour distributed biodiesel production over large-scale continuous processes when the size of the market, distance, cost of feedstock, and its availability are taken into account.[9]

The most relevant operating parameters affecting the yield and conversion in the transesterification reactor are catalyst concentration, reaction temperature, alcohol-to-oil ratio, and reaction time. The optimal operating conditions depend on the nature of the feedstock, especially physicochemical properties affecting the kinetics of the reactions. These properties are related to the triglyceride composition of the feedstock, which varies considerably among different sources of raw material. Inherent uncertainties associated with this variability may significantly affect process yield and economics. Thus, the optimal operating conditions could vary among different feedstock sources.[3] Raw material variability needs to be taken into account in order to guarantee a competitive production process.

The qualitative effects of relevant process variables for optimization have been experimentally assessed for different raw materials.[3,10] For example, both a high catalyst load and high reaction temperature give almost complete triglyceride conversion, but an excess in any of these process variables favours the undesirable saponification reaction, which reduces the ester yield. The same applies for reaction times: long reaction times ensure conversion of triglycerides, but since product losses due to saponification are inevitable, an excess in the duration of a production run will necessarily lower the yield of the process. Thus, the biodiesel reactor should be optimally operated to ensure that triglycerides are converted with a high ester yield. In this work, a run-to-run optimization methodology is proposed to deal with feedstock variability in the biodiesel transesterification step. The methodology combines model-based optimization and optimal experimental design with active learning in data gathering, using probabilistic tendency models as predictive tools to improve ester yield after a few production runs. In each run, only a few samples are taken, and a few species are measured. This makes the proposed methodology very appealing for its applications to industrial environments.

BIODIESEL REACTOR MODELLING

Triglycerides are the principal component of common vegetable oils and animal fats. These are esters of fatty acids with glycerol. Triglycerides can react with alcohol in a typical transesterification process.[1] The global transesterification reaction is:

$$Triglyceride + 3Alcohol \leftrightarrow Glycerol + 3Ester \quad (1)$$

* *Author to whom correspondence may be addressed.*
E-mail address: ecmarti@santafe-conicet.gov.ar
Can. J. Chem. Eng. 93:1613–1623, 2015

DOI 10.1002/cjce.22249
Published online 16 July 2015 in Wiley Online Library (wileyonlinelibrary.com).

In this reaction system, triglycerides react with alcohol to produce alkyl ester and diglycerides. Diglycerides react with alcohol too, yielding alkyl ester and monoglycerides. Finally, monoglycerides and alcohol react, producing alkyl ester and glycerol. A catalyst is usually used to promote the forward reaction rate and improve its yield. An excess of alcohol is used to increase the reaction rate and to shift the equilibrium towards the biodiesel production side. Methanol and ethanol are frequently used, especially the former since its cost is lower and it has better physical and chemical properties for the reaction of interest. In the alkali-catalyzed transesterification process, the catalyst may also react with biodiesel and glycerides to form soap. Equation (2) corresponds to the saponification reaction, where the catalyst (sodium hydroxide) reacts with esters, forming soap and alcohol:

$$Ester + NaOH \rightarrow Alcohol + Soap \tag{2}$$

This undesirable reaction lowers the yield of the biodiesel and generates soap, which makes the separation process more difficult and costly.

Transesterification and saponification kinetics[11] in the left part of Table 1 correspond to the set of reactions. Saponification reactions of glycerides and esters are included since they are instrumental to properly describing the influence of the temperature profile and catalyst load on the product yield of a batch biodiesel production process. In the right part of Table 1, the reaction rates r_i of alternative reaction pathways are given. Each reaction has an associated intrinsic kinetic rate k_i which in turn depends on two parameters through the well-known Arrhenius equation:

$$k_i = A_i e^{-B_i/T} \tag{3}$$

where A_i is the pre-exponential factor; B_i is the quotient between the activation energy of the reaction and the universal gas constant R; and T is the absolute temperature. The values of parameters A_i and B_i strongly depend on the feedstock source (kind and composition of triglycerides, impurities, water content, etc.), but to the best of our knowledge there is no model or correlation in the existing literature that explicitly relates the feed composition to the kinetic parameters. Moreover, the detailed composition of the triglycerides present in the feedstock source is not usually known in industrial environments.

Batch homogeneous transesterification with an alkali catalyst is the technology of choice for biodiesel production. Methanol and sodium hydroxide are the most used alcohol and catalyst. Triglycerides may come from different feedstock sources: soybean oil, sunflower oil, animal fat, etc. It is assumed here that the nature of the triglycerides will not vary erratically but from time to time as the source of raw material changes, which gives enough room to optimize the process over a number of runs. All reagents are mixed and preheated, and the mixture is then charged to a batch reactor equipped with a heat exchanger device (coil and/or jacket) and an agitator. The reaction takes place for a fixed amount of time, and then the products and the unreacted reagents go to the separation processes (decantation, washing, distillation, etc). Even though the stoichiometry from alcohol to oil is 3:1, usually a ratio of 6:1 is used in order to shift the reaction to the product side. By assuming perfect mixing and vigorous agitation in the batch reactor, mass transfer limitations can be neglected.[12] Physicochemical properties are assumed constant along each run. Bearing in mind this hypothesis, the dynamics for a batch reactor can be described by mass balances as follows:

$$\frac{d[TG]}{dt} = -r_1 + r_2 - r_7$$

$$\frac{d[DG]}{dt} = r_1 - r_2 - r_3 + r_4 + r_7 - r_8$$

$$\frac{d[MG]}{dt} = r_3 - r_4 - r_5 + r_6 + r_8 - r_9$$

$$\frac{d[E]}{dt} = r_1 + r_3 + r_5 - r_2 - r_4 - r_6 - r_{10} \tag{4a}$$

$$\frac{d[CH_3OH]}{dt} = -\frac{d[E]}{dt}$$

$$\frac{d[G]}{dt} = r_5 - r_6 + r_9$$

$$\frac{d[OH]}{dt} = -r_7 - r_8 - r_9 - r_{10}$$

where brackets stand for species molar concentrations, and the abbreviations *TG*, *DG*, *MG*, and *G* refer to triglycerides, diglycerides, monoglycerides, and glycerol, respectively. *E* stands for methyl ester (biodiesel), *OH* for hydroxide ion (catalyst), and CH_3OH for methanol.

The energy balance can be described by:

$$\rho C_p \frac{\partial T}{\partial t} = Q_X - \sum_i r_i \Delta H_i \tag{4b}$$

where ρ stands for density, C_p for heat capacity, ΔH_i for enthalpy changes involved in the ith reaction, and Q_X refers to the heat exchanged through a coil or jacket per unit of time and volume. It should be pointed out that the initial concentrations for all species and the reactor temperature must be known for integrating the system of equations in (4).

In this work, the experiments are simulated using this model, called the in silico model, which will be used as a proxy for the actual process to simulate experimental data that may be sampled in a biodiesel production run. The structure and parameters are considered unknown when the run-to-run optimization methodology is applied, and only simulated sampled data are used in the examples in the Simulation Modelling section. There is no reliable and comprehensive information about kinetic and thermodynamic parameters for all the transesterification and saponification

Table 1. Reactions and their rate expression for the *in silico* model

Reaction pathway	Rate expression
$TG + CH_3OH \rightarrow DG + E$	$r_1 = k_1[OH][TG][CH_3OH]$
$DG + E \rightarrow TG + CH_3OH$	$r_2 = k_2[OH][DG][E]$
$DG + CH_3OH \rightarrow MG + E$	$r_3 = k_3[OH][DG][CH_3OH]$
$MG + E \rightarrow DG + CH_3OH$	$r_4 = k_4[OH][MG][E]$
$MG + CH_3OH \rightarrow G + E$	$r_5 = k_5[OH][MG][CH_3OH]$
$G + E \rightarrow MG + CH_3OH$	$r_6 = k_6[OH][G][E]$
$TG + OH \rightarrow S + DG$	$r_7 = k_7[OH][TG]$
$DG + OH \rightarrow S + MG$	$r_8 = k_8[OH][DG]$
$MG + OH \rightarrow S + G$	$r_9 = k_9[OH][MG]$
$E + OH \rightarrow S + CH_3OH$	$r_{10} = k_{10}[OH][E]$

Table 2. *In silico* model parameterizations for different feedstocks

Parameter	Units	*Feedstock 1*	*Feedstock 2*	*Feedstock 3*
A_1	$[L^2 \cdot mol^{-2} \cdot min^{-1}]$	4.2447×10^8	3.6871×10^8	1.3067×10^8
A_2	$[L^2 \cdot mol^{-2} \cdot min^{-1}]$	2.1754×10^6	1.1052×10^6	3.3646×10^6
A_3	$[L^2 \cdot mol^{-2} \cdot min^{-1}]$	5.7097×10^{12}	8.4468×10^{12}	4.1139×10^{12}
A_4	$[L^2 \cdot mol^{-2} \cdot min^{-1}]$	1.0824×10^{10}	2.5756×10^{10}	9.1583×10^9
A_5	$[L^2 \cdot mol^{-2} \cdot min^{-1}]$	1.7355×10^6	1.1658×10^6	1.8115×10^6
A_6	$[L^2 \cdot mol^{-2} \cdot min^{-1}]$	2.5186×10^6	3.0964×10^6	2.0566×10^6
A_7	$[L \cdot mol^{-1} \cdot min^{-1}]$	5.8674×10^9	2.3126×10^9	2.2848×10^5
A_8	$[L \cdot mol^{-1} \cdot min^{-1}]$	4.7867×10^9	4.0460×10^9	3.6823×10^9
A_9	$[L \cdot mol^{-1} \cdot min^{-1}]$	1.5580×10^9	8.5888×10^8	1.2236×10^9
A_{10}	$[L \cdot mol^{-1} \cdot min^{-1}]$	3.8596×10^9	4.9473×10^9	2.9874×10^9
B_1	[K]	6594.1	6629.4	6516.5
B_2	[K]	4952.3	4803.4	5168.5
B_3	[K]	9537.8	9747.7	9511.8
B_4	[K]	8073.3	8430.9	8091.7
B_5	[K]	4479.0	4429.9	4574.5
B_6	[K]	5668.3	5809.2	5675.0
B_7	[K]	8871.9	8571.8	5314.4
B_8	[K]	8074.7	8024.9	7994.0
B_9	[K]	7396.4	7206.4	7322.4
B_{10}	[K]	7873.5	7960.3	7794.8

reactions. Three arbitrary sets of kinetic parameters are given in Table 2, describing different dynamic behaviours corresponding to different feedstock sources (namely feedstocks 1, 2, and 3). These may correspond to different oils, fats, and/or mixtures. The corresponding enthalpies for each reaction and the product ρC_p are given in Table 3. They are only provided here in order to reproduce experimental data reported in the related literature.[3]

In Figure 1, the contour levels for the performance index (ester yield) for feedstock 1 are shown for the case of a constant temperature profile. The alcohol-to-oil molar ratio is 6:1, and the reaction time is 60 min. It is worth highlighting that catalyst concentration has a far stronger influence than temperature in defining the yield levels.

Different dynamic behaviours can be reproduced with this model, depending on the values of parameters used in the reaction rate expressions. In Figure 2, the influence on ester yield of temperature (for a catalyst concentration of 0.2 mol/L) and of catalyst (for a temperature of 50 °C) for feedstocks 1 and 2 are compared. As can be seen, the optimal setting for these variables heavily depends on model parameters, which in turn reflect the inherent variability of alternative raw materials. For a producer that gets feedstock from different sources, the dynamic behaviour of the transesterification reactor may vary considerably when changing from one feedstock source to another. As a result of this uncertainty, run-to-run optimization is necessary to achieve near-optimal yield in biodiesel production. Every time that the feedstock is changed, the methodology can be applied again to obtain the new optimal policy (it is assumed that the physico-chemical properties do not vary significantly within the same feedstock).

Both the number of parameters involved and lacking the needed measurements would prevent using the in silico model for productivity optimization. In a production run, both the methyl ester and hydroxide concentrations can be inferred reliably with the standard analytical methods available, i.e. infrared spectroscopy and volumetric titration. This avoids the use of chromatography, which is both expensive and time-consuming. Using only these available measurement methods, tendency models are proposed to optimize productivity. A tendency model is a simplified nonlinear model of a process that combines data with fundamental knowledge of the process characteristics.[13–19]

Models based only on first principles often fail to extrapolate away from the conditions where they were developed, usually due to parametric and structural errors. As a result, optimization

Table 3. Thermal parameters for two different feedstocks

Parameter	Units	*Feedstock 1*	*Feedstock 3*
ΔH_1	$[J \cdot mol^{-1}]$	1.3649×10^4	1.1207×10^4
ΔH_2	$[J \cdot mol^{-1}]$	-1.3649×10^4	-1.1207×10^4
ΔH_3	$[J \cdot mol^{-1}]$	1.2175×10^4	1.1806×10^4
ΔH_4	$[J \cdot mol^{-1}]$	-1.2175×10^4	-1.1806×10^4
ΔH_5	$[J \cdot mol^{-1}]$	-0.9888×10^4	-0.9150×10^4
ΔH_6	$[J \cdot mol^{-1}]$	0.9888×10^4	0.9150×10^4
ΔH_7	$[J \cdot mol^{-1}]$	-1.0393×10^4	-1.0334×10^4
ΔH_8	$[J \cdot mol^{-1}]$	-1.0808×10^4	-1.0900×10^4
ΔH_9	$[J \cdot mol^{-1}]$	-0.9977×10^4	-0.9960×10^4
ΔH_{10}	$[J \cdot mol^{-1}]$	-1.0808×10^4	-1.0833×10^4
ρC_p	$[J \cdot m^{-3} \cdot K^{-1}]$	1.76×10^6	

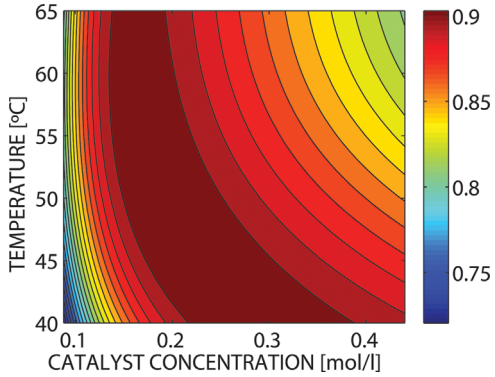

Figure 1. Performance contour levels of the *in silico* model for feedstock 1.

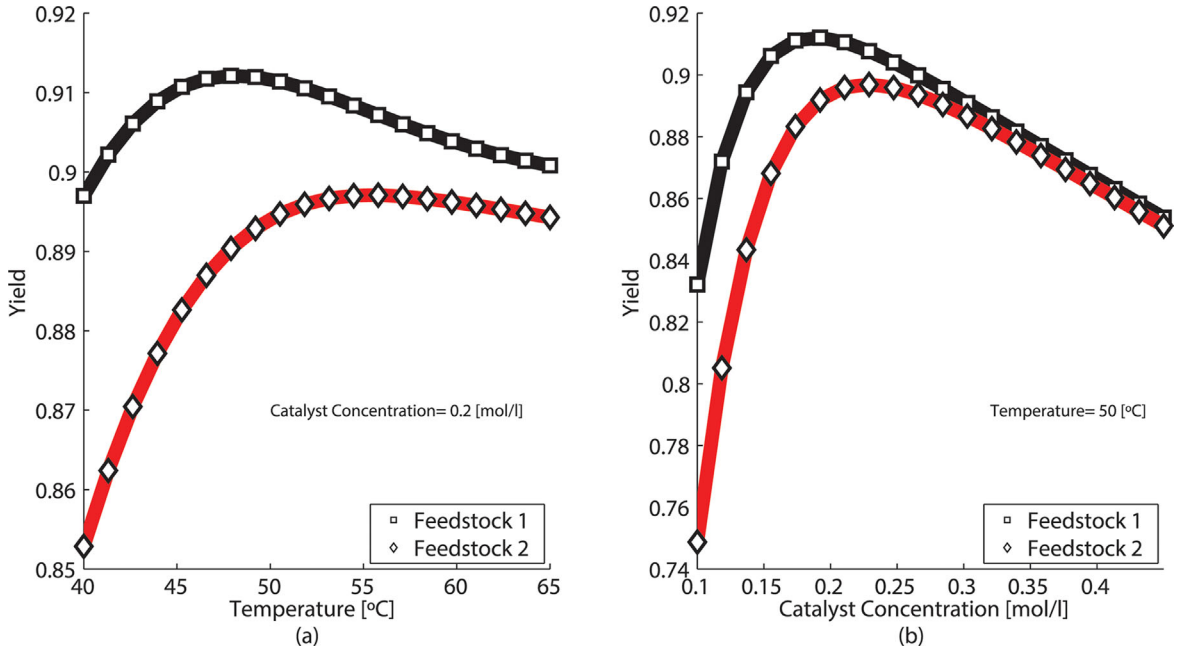

Figure 2. Influence of process variables on the transesterification reaction yield for two different feedstocks: (a) temperature, (b) initial catalyst concentration.

methodologies based on these models may not guarantee a productivity improvement. In the *modelling for optimization* framework, models are used as tools to increasingly improve process performance, instead of being mathematical devices for describing or explaining behaviour over a wide range of operating conditions. It is assumed that the model has structural and parametric mismatch with the real process, but this is not important as long as the model captures the tendency of the process performance for changing the operating policy. Notice that the focus of interest is not related to improving precision of model parameters, but in optimizing the operating policy parameters. Modelling for optimization is necessarily of an iterative nature, since model update – as more experimental data are gathered – and operating condition optimization are tightly coupled.[20,21]

A tendency model combines fundamental first-principles knowledge and constitutive laws with sampled data from the real plant. Tendency models are of low complexity so they can be updated after each run as the operating conditions change and new data are available. In the biodiesel production process, it is necessary that the model takes into account both transesterification and saponification reactions, since without the latter, the tendency model will not be able to predict the performance decrease due to an excess of catalyst. The dependence of kinetic parameters on temperature is also mandatory in order to avoid too-high temperature levels where saponification reactions may give rise to unacceptable levels of product losses that lower process productivity.

In this work, the tendency model for optimization of biodiesel production is based on an aggregate direct transesterification reaction and saponification of the lump of triglycerides and the ester using the reactions and rate expressions in Table 4. It is noteworthy that the tendency model has only 6 parameters compared to the 20 parameters in the in silico model. The mass balance equations for the batch reactor are:

$$\frac{d[TG]}{dt} = -r_1 - r_2$$

Table 4. Tendency model reactions and their rate expressions

Lumped reaction	Rate expression
$TG + 3CH_3OH \rightarrow G + 3E$	$r_1 = k_1[OH][TG][CH_3OH]$
$TG + 3OH \rightarrow G + 3S$	$r_2 = k_2[OH][TG]$
$E + OH \rightarrow S + CH_3OH$	$r_3 = k_3[OH][E]$

$$\frac{d[E]}{dt} = 3r_1 - r_3$$

$$\frac{d[CH_3OH]}{dt} = -\frac{d[E]}{dt} \qquad (5)$$

$$\frac{d[OH]}{dt} = -3r_2 - r_3$$

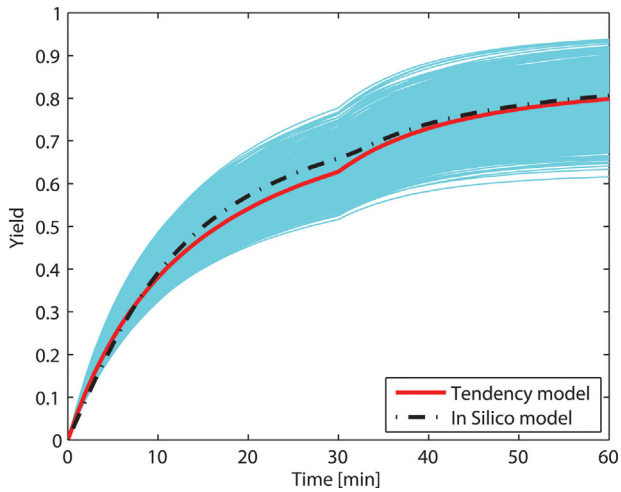

Figure 3. Prediction uncertainty in the probabilistic tendency model.

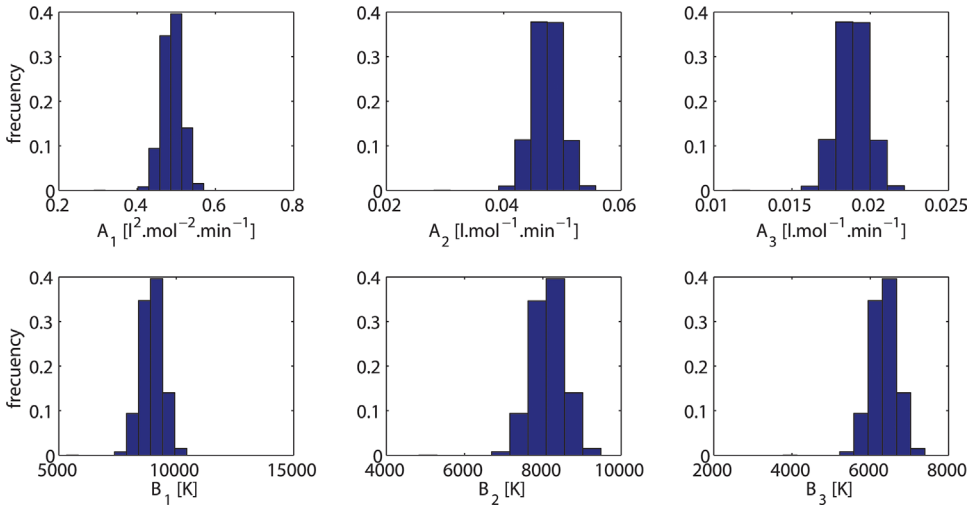

Figure 4. Histograms for the tendency model parameters.

When integrating the tendency model dynamics in Equation (5), the expression for k_i is given by Equation (3) above, and the initial concentration for each species has to be known.

In traditional tendency modelling for optimization, the process dynamics are described using a single parameter set. Probabilistic tendency models, on the other hand, are based on a Bayesian approach: the elements of the vector of model parameters $\boldsymbol{\theta}$ are not single values. Instead, they are described as stochastic variables (see Martinez et al.[19] for details). Each model parameter is actually a distribution, and uncertainty in the prediction of the model is described using the joint distribution of model parameters $p(\boldsymbol{\theta}) = \prod_i p(\theta_i)$. In Figure 3, a comparison is made, for a given operating policy, between the in silico model for feedstock 1 and a probabilistic tendency model (and its uncertainty in biodiesel time profiles predictions). The parameter distributions for the tendency model used to obtain Figure 3 are shown in Figure 4. They were fitted using intra-run sampled data. As can be seen, there exists a reasonable agreement when the expected values of tendency models predictions are considered. Light blue yield profiles probabilistically characterize the remaining uncertainty in model predictions.

Since the model parameters are represented as stochastic variables, policy parameters are also represented by statistical distributions. These distributions are of paramount importance because they give information about the remaining uncertainty in the optimal policy, the expected performance, and its sensitivity to the policy parameters. As will be shown later, the characterization of performance sensitivity is a key issue for experimental design in modelling for optimization.

RUN-TO-RUN OPTIMIZATION

The proposed methodology is schematized in Figure 5. First, an exploratory run is undertaken using an arbitrary policy. This policy is chosen based on a priori knowledge from industrial practice or laboratory and pilot plant assays. Data gathered from this exploratory run are used to obtain the first parameterization of the probability distributions for the tendency model. Using this parameterization, a model-based optimization step is carried out to find the optimal operating policy that maximizes the performance of the process. Then, the sampling times for the next experiment are designed to maximize the information content. The model-based optimized policy is evaluated experimentally and new data are obtained. The model is re-parameterized using data from the new operating condition, and a new iteration can be performed.

Usually, any model prediction loses accuracy when it is used to make predictions far away from the operating conditions where

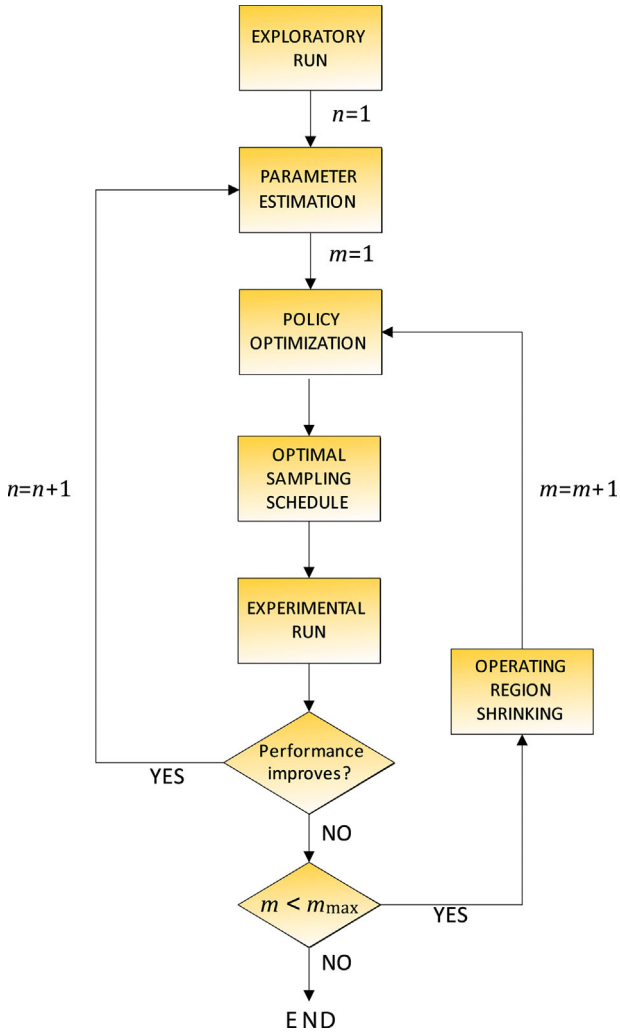

Figure 5. Run-to-run optimization using probabilistic tendency models.

model parameters were fitted. This is especially true for tendency models, which are rather simple in their structure. Then, the new operating policy could cause a performance loss when evaluated experimentally. In the proposed methodology, an adaptive procedure is used to solve this problem.[22] First, the bounds for the policy parameters in the model-based optimization problem are set over a wide range. The problem is solved using these bounds. Then the policy is tested experimentally. If the performance actually increases, the bounds are reset to their original values and a new iteration begins. If it does not increase, it is a sign that the model is failing to predict the behaviour of the process when extrapolating far away from the previous operating conditions. Then, the bounds for policy parameters are shrunk, the model-based optimization problem is performed again in a smaller region (to prevent the model having to extrapolate far away from the conditions where it was parameterized), and the new policy is evaluated experimentally. This is done without updating the model and is considered part of the same iteration. This strategy could be repeated until the performance improves or the operating region is shrunk enough, i.e. up to $m_{\max}$ times. If the performance improves, only data from the last run is used to update the model in the new iteration. If the shrinking process is performed enough times but the performance does not improve, the methodology is considered to have converged to a stationary point. The true optimal policy is chosen among all operating conditions tested. In the following subsections, each of the fundamental aspects of the methodology is discussed and explained.

It is worth noting that the objective of this run-to-run methodology is to improve the performance of the process. The convergence of the model parameter distributions is not guaranteed, but this issue is of no concern, since the model is just a tool to guide the search towards the optimum. Convergence of the methodology is based on the shrinking process which excludes the operating conditions that may cause a performance loss. If the real optimum is found, any other operating conditions would not give a better performance, and eventually the operating region will shrink around it. Otherwise, if the model fails to capture the tendency of the process with respect to the policy parameter in a certain iteration (because the structure of the model is not good enough in these operating conditions or because the sampling led to a bad parameterization), the model-based optimization may tend to move the operating condition in the direction where the performance always decreases. If that occurs, the methodology will never find a better operating condition and the region will shrink around the best policy of the last iteration, thus converging.

Bootstrapping Parameter Distributions

The tendency model must be parameterized by repeatedly solving a data fitting problem. This step is of paramount importance, because if the model fails to capture the tendency of process performance, then the run-to-run algorithm may converge to a sub-optimal policy. For a given data set, parameter estimation can be done using the traditional approaches for inverse problems. The weighted least squares method is chosen here. In biodiesel production, weighting factors w_l are chosen to favour the fitting of ester data sampled over the run as follows:

$$\min_{\boldsymbol{\theta}} J_{er}$$

$$\text{such that: } LB_\theta \le \boldsymbol{\theta} \le UB_\theta \qquad (6)$$

$$\frac{d[C]}{dt} = F(\theta, P_n, [C])$$

$$[C]_{(t=0)} = C_{to}$$

where $J_{er} = \sum_l \sum_i \left(\frac{[C_l]^{\exp}_{(t_i)} - [C_l]_{(t_i)}}{[C_l]^{\exp}_{(t_i)}} \right)^2 . w_l$, F stands for the system of Equation (3), $[C]$ for species molar concentration, and C_{to} for initial conditions. LB_θ and UB_θ are the lower and upper bounds of the parameter vector $\boldsymbol{\theta}$, and P_n is the policy used to perform the experiment. The superscript *exp* indicates experimental data, whereas subscripts l and i indicate species and corresponding times at which measurements are taken, respectively. Not all chemical species involved in the reactions need to be measured, only those needed to identify the tendency of the process performance. The experimental data used to solve (6) are those from the last run from the previous iteration, i.e. those from the best policy tried so far.

Properly solving this above optimization problem is usually very cumbersome due to the existence of many local solutions. Combining a local search method with multiple starting points (multiple shooting) or directly resorting to global optimization methods have both been proposed.[23] In order to approximate the distribution of each model parameter, a bootstrapping technique is applied. Bootstrapping artificially generates new samples using re-sampling with replacements, in order to study the system dynamics using statistical inference.[24,25] One of the uses of the method is to approximate distributions for independent statistical variables. To construct histograms for all model parameters, the original data set $\boldsymbol{x}$ is randomly sampled with replacements to generate an artificial data set $\boldsymbol{x}_1$ of the same size. This new data set is used to obtain a single parameterization of the tendency model based on (6). Artificial re-sampling is repeated up to N times using Monte Carlo simulations to obtain new artificial data sets: $\boldsymbol{x}_1, \boldsymbol{x}_2, \ldots, \boldsymbol{x}_N$. Each data set may provide a different model parameterization. Then, for each model parameter a distribution is obtained, thus completely defining the probabilistic tendency model. The procedure for bootstrapping parameter distributions is summarized in Table 5.

Before ending this section, some comments regarding the correlation between parameters are in order. As the tendency model is nonlinear, identification problems may arise when solving the problem in (6). In this case in particular, estimated values for pre-exponential factors A_i and their corresponding parameters B_i cannot be identified if the temperature along the run does not vary considerably. Since in modelling for optimization the main objective is choosing the policy parameters so as to improve the yield, there is no guarantee that the temperature excitation is sufficient to guarantee the identifiability of A_i and B_i separately. There are some approaches to circumvent this problem. One would be to not update all model parameters if the variability of the temperature is not enough, maintaining the B_i values from the previous iteration. Alternatively, a restriction to the policy optimization problem can be added so as to enforce a parameterization of the temperature profile that guarantees a minimum level of excitation. While this restriction makes the

Table 5. Pseudo-algorithm for parameter estimation and bootstrapping

Set model parameter bounds resorting to *a priori* knowledge.
Solve problem in (6) for the complete data set.
Perform boostrapping to generate *N* new artificial data sets.
Solve problem in (6) for each artificial data set to generate distributions of model parameters.

methodology more robust, in some cases it could lead to a suboptimal policy. In the present work, the first option is used.

Policy Optimization

The main goal of run-to-run optimization is to find the vector P_n of optimal parameters for the operating policy that improves the performance of the process, which is measured as the yield at the end of the run. At any time t, the yield is defined as:

$$J_{(t)} = \frac{[E]_{(t)}}{3[TG]_{(t=0)}} \tag{7}$$

Alternative performance indices can be defined to include other factors of interest that take into account the purification steps, the overall production cost, etc.

Because the tendency model loses reliability away from the operating conditions that were used to fit its parameters, an adaptive methodology is proposed to increasingly reduce the feasible region for optimization (see the Operating Region Shrinking section, below). Using a tendency model with parameters $\boldsymbol{\theta}$, the following nonlinear program (NLP) is solved:

$$\max_{P_n} J_{(tf)}$$

$$\text{such that: } LB \leq P_n \leq UB \tag{8}$$

$$\frac{d[C]}{dt} = F(\theta, P_n, [C])$$

$$[C]_{(t=0)} = C_{to}$$

where LB and UB are the lower and upper bounds of vector P_n, $[E]_{(t)}$ is methyl ester concentration at time t, tf is final time, and the rest of the variables are the same as in (6). The problem in (8) is solved using a constrained NLP solver. Since in probabilistic tendency models, uncertainty is modelled using distributions of parameters, the model-based optimization problem in (8) should be solved repeatedly to obtain distributions for the optimal values of policy parameters. To this aim, a Monte Carlo approach is used. First, the distribution for each model parameter is sampled to obtain a given realization of the vector $\boldsymbol{\theta}$. The optimization problem is solved and the corresponding optimal values of policy parameters are obtained. With data gathered in independent samples, histograms for policy parameters are obtained. The optimal policy for the next experiment is defined accordingly. Different alternatives can be chosen for defining the optimal policy: the mean, the mode, or another estimator can be taken from the policy parameter distributions. Model-based policy optimization is summarized in the pseudo-algorithm of Table 6.

Table 6. Pseudo-algorithm for policy optimization

Set the policy parameters bounds:
  If this is the first run of the iteration, reset policy parameter bounds to its initial values.
  Else, use the values calculated with algorithm in Table 8.
To generate distributions of policy parameters, *do N* times:
  Sample the model parameter distribution to generate a model parameter set.
  Solve problem in (7) using the tendency model and this parameter set.
Choose the optimal policy parameterization using these distributions.

Optimal Sampling Schedule

Data to update the tendency model in the next iteration are sampled in order to maximize the information content for performance improvement. For each run, all available sampled measurements are used. The design of the sampling schedule is done after the model-optimized policy is known, so the problem here is to pinpoint the most informative sampling times along the run. To obtain the most informative experiment, the sensitivity matrix Q is used.[18,19,26] The entries of this matrix are defined as follows:

$$Q_{ij} = SI_{ij} \tag{9}$$

where SI_{ij} are the sensitivity indices of the performance J. The subindices i and j stand for sampling time and policy parameter, respectively. Several methods are available to calculate these indices. Global methods such as the Variance method[27] and the Fast Fourier Transform method[28] are proposed in this work (which have been found to be useful when using models with less than 20 parameters). In all these methods, the sensitivity indices are defined as follows:

$$SI_{ij} = \frac{V_{ij}}{V_i} \tag{10}$$

V_{ij} and V_i are the conditional and total variance of the performance J, calculated accordingly to Equation (7). SI_{ij} can be interpreted as the fraction of the uncertainty in the performance prediction that is related to the jth policy parameter for the ith sampling time.

To find the optimal sampling schedule, the sampling vector is defined as $ts = [ts_1, \ldots, ts_i, ts_{i+1}, \ldots, ts_f]$, whose entries are the variables to be optimized. Each potential sampling time vector has a different sensitivity matrix Q. The problem formulation for optimal sampling is based on the well-known D-criterion used for optimal design of experiments:[29]

$$\max_{ts} det(Q^T.Q)$$

$$\text{such that: } ts_{\min} \leq ts_1 \tag{11}$$

$$\Delta t \leq ts_{i+1} - ts_i$$

$$ts_f \leq ts_{\max}$$

where $ts_{\min}$ and $ts_{\max}$ are the minimum and maximum allowable values of the elements of ts, and Δt is the minimum elapsed time between samples. The number of sampling times which must be chosen in each experiment is limited by the available budget for processing samples. The whole procedure is presented in the pseudo-algorithm of Table 7.

Table 7. Pseudo-algorithm for sampling time scheme

Solve problem in (11) calculating det $(Q^T.Q)$as follows:
For a given sampling time vector ***ts***, *perform* a global sensitivity analysis (GSA) of the policy parameters at each element of the time vector, using the policy parameter distributions and the most probable parameterization of the tendency model.
Calculate matrix ***Q*** using the *SI* from the GSA.
Calculate the determinant *det* $(Q^T.Q)$.
The vector ***ts*** that maximizes *det* $(Q^T.Q)$ is the optimal sampling time vector.

Operating Region Shrinking

After the new policy is calculated and the next experiment has been designed, a new run is performed and samples are taken. If the process performance improves compared with the previous iteration, a new iteration of the algorithm is undertaken. If the performance decreases, a second loop is activated: a new policy optimization is performed, but in a smaller operating region. The feasible region for model-based optimization that contains the policy previously found is then conveniently shrunk. A summary of the procedure is given in the pseudo-algorithm of Table 8. Here, m is the iteration number for the second loop, $P_{n-1(j)}$ is the policy found in the previous iteration, $P^{*}_{n(j)}$ is the policy tried in the previous run (which gives a yield decrease), $LB_{m(j)}$ and $UB_{m(j)}$ are the lower and upper bounds for the optimization problem, and sf is the shrinking factor. The jth subindex stands for each element of the policy parameters vector. In Figure 6, a schematic representation of shrinking the operating policy for a two-parameter policy is given.

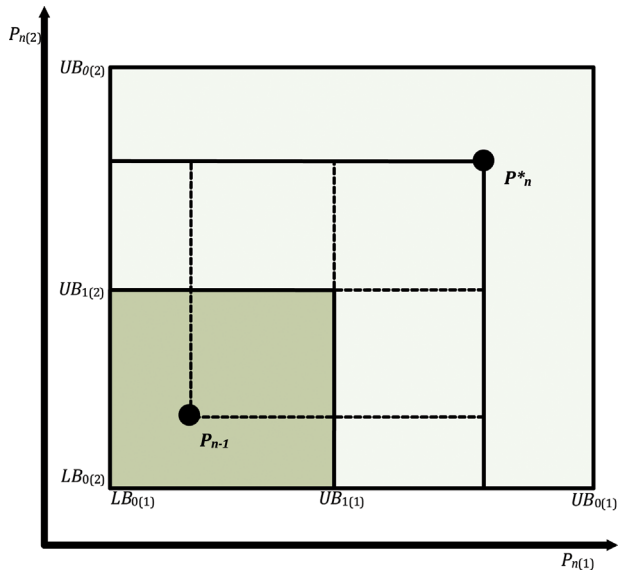

Figure 6. Schema for shrinking the operating region in a two-parameter policy space.

SIMULATION RESULTS

Using data generated with the in silico model for feedstock 1, run-to-run optimization based on the algorithm in Figure 5 was carried out. Normally-distributed measurement errors with mean = 0 and a standard deviation of 5 % are added to the simulated data. The operating policy is defined by four parameters: initial concentration for the catalyst $[OH]_{to}$, plus three parameters for describing a temperature step profile: two temperature levels $T_1$and T_2' and the switching time t_{SW} between them. The temperature profile is chosen as a single step for the sake of simplicity. Other parameterizations could be chosen, but as can be seen in Figure 1, the most important factor is the catalyst load.

The heat exchanged in the in silico model is described by:

$$Q_X = UAv(T_X - T)$$

$$T_{sp} = \begin{cases} T_1 \; if \; t < t_{SW} \\ \qquad\qquad T_X = 30\,(T_{sp} - T) + 323 \\ T_2 \; otherwise \end{cases} \tag{12}$$

$$293\ \text{K} \le T_X \le 373\ \text{K}$$

where T_X is the temperature of the fluid in the heat exchanger device, T_{sp} is the temperature setpoint, and UAv is the heat transfer coefficient per unit of volume: $1.14\ 10^5 \text{J} \cdot \text{min}^{-1} \cdot \text{K}^{-1} \cdot \text{m}^{-3}$.

Data sampled are methyl ester and hydroxide ion concentrations, and their corresponding weighting factors w_l were chosen to be 0.8 and 0.2, respectively. The number of sampling times is set to 4 (plus the ones at the initial and final times) and $ts_{\min}$, $ts_{\max}$, and Δt parameters for the problem in (11) are set to 4, 56, and 4 min, respectively. The shrinking factor is chosen as 0.5.

The duration of the run is set to 60 min and the methanol-to-oil molar ratio is chosen as 6:1. Except for the catalyst concentration, initial conditions are the same for all runs, where triglyceride and methanol initial concentrations are set to 0.8 and 4.8 mol/L, respectively. Initial concentrations for other species are 0 mol/L. Bounds for the policy parameters are as follows: [0.088;0.44] mol/L for $[OH]_{to}$, [4;56] min for t_{SW}, and [40;65] °C for both temperature levels. The maximum number of runs $m_{\max}$ in each iteration of the optimization procedure in Figure 5 is set to 4.

In this work, all calculations are performed in MATLAB 7.6 (R2008a). Problems in (6, 8, 11) are solved using a sequential quadratic programming approach, by combining the fmincon solver for optimization and the ode15s solver for integrating the ordinary differential equation system. To avoid local optima, the optimization algorithm is initialized from different starting points and the best value of the objective function found is selected as the optimum.

For the sensitivity indices, the FAST method is used. To approximate the overall effect, each index is defined as the summation of the first and all second global sensitivity indices. Calculations are done with the algorithm developed by Plischke.[28] Solving the problem in (11) requires computing the SI for each policy parameter at each entry of the optimization vector ts. This is very cumbersome, since for every evaluation of the objective function for the problem in (11) the FAST method has to be used. To solve this issue, the following approach is proposed: the FAST method is applied at selected arbitrary sampling times (in this paper, 10 equidistant sampling times). SI for different sampling times are approximated using spline-based interpolators.

The minimum temperature step change for updating B_i parameters is 2 °C. With a lower temperature step, an identification problem may arise, so only A_i parameters are updated whereas B_i parameters are taken from the previous iteration. With a higher temperature step change, the covariance of the parameters is nearly zero, even when the switching time t_{SW} is near its upper bound (which implies a short duration of the final part of the temperature profile).

Table 8. Pseudo-algorithm for operating region shrinking

For each element of the proposed optimal policy parameter vector $P^{*}_{n(j)}$

If the element of the proposed policy is less than the corresponding element of the previous iteration optimal policy $P_{n-1(j)}$, set the new bounds as follows:

$LB_{m(j)} = P_{n-1(j)} + \left(P^{*}_{n(j)} - P_{n-1(j)}\right) sf \; UB_{m(j)} = UB_{m-1(j)}$

If the element of the proposed policy is greater than the corresponding element of the previous iteration optimal policy $P_{n-1(j)}$, set the new bounds as follows:

$UB_{m(j)} = P_{n-1(j)} + \left(P^{*}_{n(j)} - P_{n-1(j)}\right) sf \; LB_{m(j)} = LB_{m-1(j)}$

Table 9. Results obtained in run-to-run optimization using data simulated with the *in silico* model for feedstock 1

		Policy				
		$[OH]_{to}$	t_{sw}	T_1	T_2	
ITER #	Run #	[mol·L^{-1}]	[min]	[°C]	[°C]	Yield
0	1	0.100	30.00	40.00	45.00	0.7862
1	2	0.118	7.11	65.00	65.00	0.8844
2	3	0.165	30.43	65.00	64.92	0.9088
3	4	0.171	17.24	64.68	40.35	0.9115
4	5	0.180	13.86	40.01	40.06	0.8881
	6	0.176	15.55	52.34	40.21	0.9062
	7	0.173	16.41	58.57	42.88	0.9115
	8	0.172	27.15	61.62	41.54	0.9120
5	9	0.169	26.77	40.13	57.84	0.9087
	10	**0.181**	**49.84**	**50.88**	**49.64**	**0.9121**
6	11	0.218	43.56	40.09	59.90	0.9091
	12	0.200	46.72	45.51	54.75	0.9111
	13	0.190	48.74	48.21	52.16	0.9117
	14	0.186	55.96	51.04	50.90	0.9121
InS	-	***0.193***	***31.71***	***53.26***	***40.00***	***0.9131***

Results obtained in each iteration of the algorithm are reported in Table 9, along with the corresponding in silico optimum (***InS***). The first exploratory run is designed arbitrarily and no parameterization of the model was used to design this experiment. Only the a priori knowledge of the lower and upper bounds for the parameters is needed in the exploratory run. In Iteration #6, after reaching the maximum number of runs, a lower yield than the previous one (Iteration #5) is obtained. This implies that the run-to-run algorithm has reached the neighbourhood of a stationary point of the objective function. Then, the optimal policy is the one highlighted for Iteration #5–Run #10 in Table 9. It is worth noting that the yield loss regarding the optimal policy (from the in silico model) is less than 1%. In Figure 7, the model-based optimized temperature profile for Iteration #5–Run #10 is shown along with optimal sampling times. For this policy, ester and hydroxide concentrations predicted by the tendency model with its most probable parameterization are given in Figure 8.

The learning curve for the complete process is shown in Figure 9. The drop of the yield in some runs corresponds to extrapolations where the model failed to predict the performance of the process, mainly because the new operating point is somewhat distant from the previous one. After such a drop, the operating region is shrunk to a smaller region, and the yield may increase. The region is increasingly shrunk until a yield improvement is achieved (and a new iteration begins) or until the region has been shrunk a number of times so that the stopping criterion is fulfilled. As the run-to-run optimization methodology is biased to explore only the most profitable region of operating conditions, it is very appealing for industrial applications.

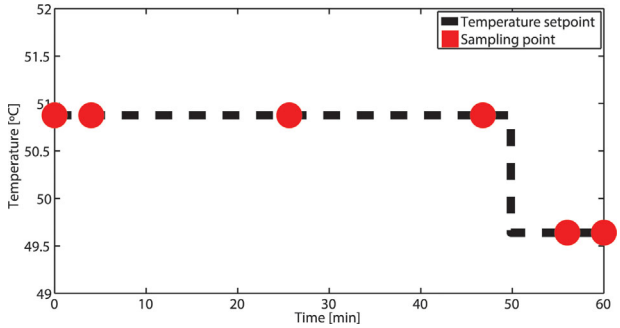

Figure 7. Optimal temperature profile and sampling times for Iteration #5–Run #2 using simulation data from feedstock 1.

In order to study the suitability of the methodology for dealing with feedstock variability, the in silico model parameterization has been changed from feedstock 1 to feedstock 3. This change accounts for a different source of triglycerides in the feedstock (i.e. changing from one type of oil to another). The optimal operating policy is different now, and the algorithm in Figure 5 should be applied again. The same conditions from the previous case are maintained, but instead of an exploratory run, the optimal policy previously found by the run-to-run optimization algorithm is used in the first run. Results are given in Table 10, and the learning curve is shown in Figure 10. The policy chosen is the one from Iteration #3–Run #4. As can be seen, the proposed methodology quickly evolves to a near-optimal situation: it reaches the experimental optimum in the third iteration, and the runs from the following iteration cannot improve the yield, which stops the run-to-run optimization strategy. The yield loss with regards to the in silico model optimum is less than 1%.

The preceding results demonstrate that the proposed run-to-run optimization methodology quickly converges to a near-optimal policy using sampled data. Additionally, it performs most runs near the optimum, so the overall costs along the learning curve are relatively low (mainly due to the shrinking of the operating region near the optimal conditions). This has proven to be useful for either obtaining the optimal policy for a completely unknown

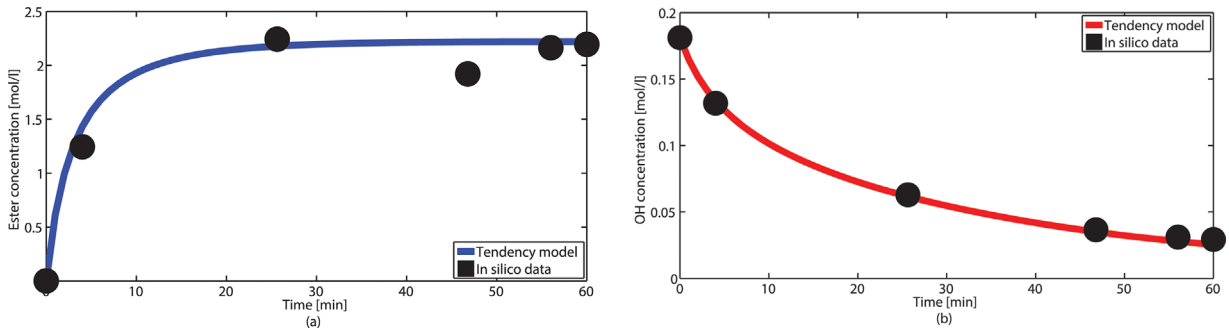

Figure 8. Concentration profiles for Iteration #5–Run #2 using simulation data from feedstock 1: (a) ester concentration profile, (b) hydroxide concentration profiles.

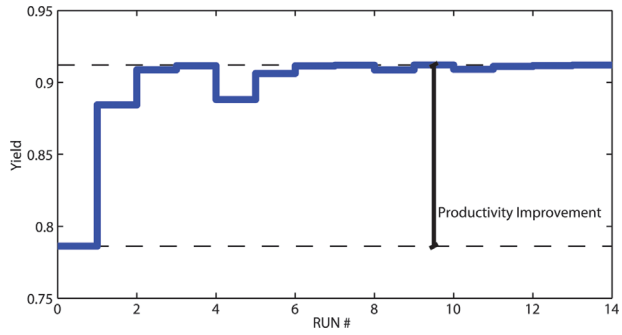

Figure 9. Learning curve for the optimization methodology applied to feedstock 1.

Table 10. Results obtained in run-to-run optimization using data simulated with the *in silico* model for feedstock 3

		Policy				
		$[OH]_{to}$	t_{SW}	T_1	T_2	
ITER #	Run #	[mol · L^{-1}]	[min]	[°C]	[°C]	Yield
0	1	0.181	49.84	50.88	49.64	0.7615
1	2	0.326	14.77	40.06	63.90	0.8336
2	3	0.315	4.00	40.69	65.00	0.8386
3	**4**	**0.287**	**34.60**	**65.00**	**64.99**	**0.8416**
4	5	0.293	52.00	65.00	40.77	0.8414
	6	0.290	43.24	65.00	64.98	0.8415
	7	0.288	17.64	65.00	64.99	0.8415
	8	0.288	30.38	65.00	64.99	0.8416
InS	-	***0.289***	***34.16***	***65.00***	***40.00***	***0.8417***

feedstock, or finding the new one following a change in the triglyceride source (both typical problems in biodiesel production). Another advantage of the methodology is that it can be applied with minimum a priori knowledge about the quantitative behaviour of the biodiesel production dynamics. This is very desirable, because in industrial practice, there is hardly ever enough time to perform comprehensive laboratory or pilot plant tests to obtain the optimal conditions for an unknown feedstock before production runs are carried out (and nothing guarantees that the obtained optimal conditions will be the same for the industrial process).

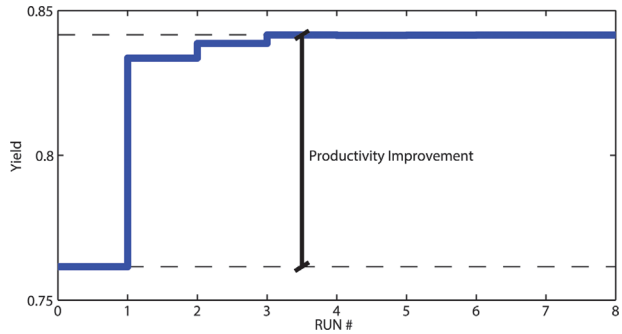

Figure 10. Learning curve following a feedstock change from feedstock 1 to feedstock 3.

CONCLUSIONS

In this work, a probabilistic tendency model for the hydroxide-catalyzed transesterification of triglycerides to produce biodiesel (which also accounts for saponification reactions) has been proposed. To the best of our knowledge, there are no previous works related to the development and use of low-complexity first-principle models (tendency models) for optimization of biodiesel production yield. Moreover, the proposed Bayesian setting for integrating experimentation with imperfect models is a novel concept for defining a sequence of runs aimed at increasingly optimizing biodiesel yield, which can also be applied to other transesterification processes such as acid-catalyzed biodiesel synthesis or when using a heterogeneous catalyst. To formulate the optimal sampling strategy in each dynamic experiment as an optimization program, a global sensitivity analysis has been proposed to pinpoint optimally informative sampling times at which process performance is most sensitive to policy parameters. Run-to-run optimization based on the probabilistic tendency model demonstrates fast convergence to a significantly improved yield in biodiesel production. Results obtained for two alternative parameterizations for the in silico model demonstrate that despite the possibility of errors in the tendency model structure and reduced information content in samples, a significant increase in biodiesel production can be achieved using model-based run-to-run optimization.

For run-to-run optimization, bootstrapping is used to re-estimate parameter distributions in a probabilistic model of biodiesel production using data gathered as the operating condition is increasingly biased towards optimal operation. Accordingly, a probabilistic tendency model is instrumental for facing the variability in composition and properties of raw materials used for biodiesel production. Additionally, repeatedly shrinking the operating region has been proposed to safely explore locally in the direction of improvement under uncertainty. The probabilistic nature of the tendency model makes the most of scarce data to successfully guide run-to-run optimization and to help avoid sensible losses in a biodiesel production reactor subjected to feedstock variability.

NOMENCLATURE

A	pre-exponential factor
B	scaled activation energy (K)
$[C]$	molar concentration for species C (mol · L^{-1})
C_p	heat capacity (J · kg^{-1} · K^{-1})
C_{to}	vector of initial concentrations (mol · L^{-1})
J	performance objective function
J_{er}	parameter estimation objective function
k	intrinsic kinetic rate
LB	vector of lower bounds for policy parameters
LB_θ	vector of lower bounds for model parameters
$p(\cdot)$	probability distribution function
$[OH]_{to}$	initial hydroxide concentration (mol · L^{-1})
P_n	vector of policy parameters for iteration n
P_n^*	proposed policy that failed to improve the yield
Q	sensitivity matrix
Q_x	heat exchanged per unit of time and volume (J · min^{-1} · m^{-3})
r	reaction rate (mol · L^{-1} · min^{-1})
SI	sensitivity index
sf	shrinking factor
T	reactor temperature (K)

T_X temperature of the fluid in the heat exchanger device (K)
T_{sp} temperature set-point (°C)
T_1 first set-point in the temperature profile (°C)
T_2 second set-point in the temperature profile (°C)
t time (min)
tf final time (min)
ts vector of sampling times (min)
t_{SW} switching time for the temperature profile (min)
UAv heat transfer coefficient per unit of volume ($J \cdot min^{-1} \cdot K^{-1} \cdot m^{-3}$)
$\boldsymbol{UB}$ vector of upper bounds for policy parameters
$\boldsymbol{UB_\theta}$ vector of upper bounds for model parameters
V_{ij} conditional variance for parameter j at time i
V_i total variance at time i
w weighting factor for parameter estimation

Greek Letters

ΔH enthalpy change ($J \cdot mol^{-1}$)
Δt minimum time distance between successive samples (min)
ρ density ($kg \cdot m^{-3}$)
$\boldsymbol{\theta}$ vector of model parameters

Chemical Species

TG triglycerides
DG diglycerides
MG monoglycerides
G glycerol
CH_3OH methanol
E methyl ester
OH hydroxide ion

REFERENCES

[1] F. Ma, M. A. Hanna, *Bioresource Technol.* **1999**, *70*, 1.
[2] D. Y. C. Leung, Y. Guo, *Fuel Process. Technol.* **2006**, *87*, 883.
[3] T. Eevera, K. Rajendran, S. Saradha, *Renew. Energ.* **2009**, *34*, 762.
[4] P. T. Benavides, U. Diwekar, *Fuel* **2013**, *103*, 585.
[5] A. Abuhabaya, J. Fieldhouse, D. Brown, *Fuel* **2013**, *103*, 963.
[6] B. L. Salvi, N. L. Panwar, *Renew. Sust. Energ. Rev.* **2012**, *16*, 3680.
[7] D. Y. C. Leung, X. Wu, M. K. H. Leung, *Appl. Energ.* **2010**, *87*, 1083.
[8] G. Vicente, M. Martínez, J. Aracil, *Bioresource Technol.* **2004**, *92*, 297.
[9] P. T. Benavides, J. Salazar, U. Diwekar, *Environ. Prog. Sustain. Energy* **2013**, *32*, 1.
[10] P. Patil, S. Deng, *Fuel* **2009**, *88*, 1302.
[11] K. Komers, F. Skopal, R. Stloukal, J. Machek, *Eur. J. Lipid Sci. Tech.* **2002**, *104*, 728.
[12] F. A. Fonseca, J. A. Vidal-Vieira, S. P. Ravagnani, *Bioresource Technol.* **2010**, *101*, 8151.
[13] D. Bonvin, D. Rippin, *Chem. Eng. Sci.* **1990**, *45*, 3417.
[14] C. Filippi, J. Bordet, J. Villermaux, S. Marchal-Brassey, C. Georgakis, *Comp. Chem. Eng.* **1989**, *13*, 35.
[15] J. Fotopoulos, C. Georgakis, H. G. Stenger Jr., *Chem. Eng. Process.* **1998**, *37*, 545.
[16] G. Georgakis, *Entropy* **1995**, *194*, 34.
[17] J. Uhlemann, M. Cabassud, M. LeLann, E. Borredon, G. Cassamatta, *Chem. Eng. Sci.* **1994**, *49*, 3169.
[18] E. C. Martínez, M. Cristaldi, R. Grau, *Ind. Eng. Chem. Res.* **2009**, *48*, 3453.
[19] E. C. Martínez, M. Cristaldi, R. Grau, *Comp. Chem. Eng.* **2013**, *49*, 37.
[20] B. Srinivasan, D. Bonvin, "Interplay between identification and optimization in run-to-run optimization schemes," *American Control Conference*, American Automatic Control Council, Anchorage, AK, USA, 8–10 May **2002**.
[21] B. Srinivasan, D. Bonvin, *Comp. Chem. Eng.* **2013**, *51*, 172.
[22] B. Srinivasan, D. Bonvin, "Convergence analysis of iterative identification and optimization schemes," *American Control Conference*, American Automatic Control Council, Denver, CO, USA, 4–6 June **2003**.
[23] M. Rodriguez-Fernandez, P. Mendes, J. R. Banga, *BioSystems* **2005**, *83*, 248.
[24] B. Efron, R. J. Tibshirani, *An introduction to the bootstrap*, Chapman & Hall, London **1993**.
[25] M. Joshi, A. Seidel-Morgenstern, A. Kremling, *Metab. Eng.* **2006**, *8*, 447.
[26] M. Rodriguez-Fernandez, S. Kucherenko, C. Pantelides, N. Shah, *Comput. Aided Chem. Eng.* **2007**, *24*, 63.
[27] A. Saltelli, M. Ratto, S. Tarantola, F. Campolongo, *Reliab. Eng. Syst. Safe.* **2006**, *91*, 1109.
[28] E. Plischke, *Reliab. Eng. Syst. Safe.* **2010**, *95*, 354.
[29] S. P. Asprey, S. Macchietto, *J. Process Control* **2002**, *12*, 545.

Manuscript received October 3, 2014; revised manuscript received October 20, 2014; accepted for publication October 20, 2014.